

## Study of the Signature of Solar Activity in Periodic Fluctuations Observed in Electron and ion Temperature at the Low Latitude Ionosphere.

Lalitha T. Alexander<sup>a</sup>, Nayfa Suliman Muhammed Al Atawi<sup>a</sup>,  
Hala M. Abu Mostafa<sup>a+b</sup>, George T. John<sup>c</sup>

<sup>a</sup>Department of Physics, Tabuk University, Tabuk, Saudi Arabia

<sup>b</sup>Department of Physics, Menofia University, Menofia, Egypt

<sup>c</sup>Department of Chemistry, St. John's College, Anchal, Kerala University, India

### Abstract

*The electron and ion temperatures at the upper ionosphere depends on both solar and terrestrial conditions and is found to exhibit a variety of periodic variations found in solar and terrestrial parameters like diurnal, seasonal, latitudinal and solar activity associated. Periodic fluctuations in the geomagnetic activity and ionospheric fluctuations result from the intrinsic state of the Sun, relative orientation of Earth with respect to the Sun and processes at the earth. Mainly Sun provides the driving force for all geomagnetic and ionospheric fluctuations. Observations using SROSS-C2 Satellite RPA payload during 1995-2000 provide an excellent opportunity to study the fluctuations in  $T_e$  and  $T_i$  in the upper ionosphere and to understand the dynamic process existing at all these altitudes. The spectral analysis of electron and ion temperatures using Fourier and wavelets technique reveal the presence of quasi periodicities such as 14-day, 18-day, 27-day, 55-day and 154-day, 180-day, 1-year and 1.3-year periods. The study of the characteristics of the Fourier and wavelet spectrum helps to infer prominent processes are associated with the heating of the upper ionosphere. The day time and night time values of  $T_e$  and  $T_i$  exhibit different types of characteristic variations. The wavelet spectrum explains the temporal evolution of the power of each periodicity present in the day time and night time values. The time evolutions of electron and ion temperatures are compared with that of Ap index and 10.7 cm solar radio flux.*

### 1. Introduction

The electron and ion temperatures at the upper ionosphere depends on both the solar and terrestrial conditions and is found to exhibit a variety of periodic variations found in solar and terrestrial parameters like diurnal, seasonal, latitudinal and solar activity associated variations (Brace et al., 1987; Oyama et al., 1996; Huba et al., 2000a; Schunk and Nagy., 1978; 2000). The ionosphere undergoes significant changes associated with solar variations both in radiation flux and solar wind plasma flow. Some geomagnetic and ionospheric fluctuations result from variations in the intrinsic state of the Sun. The solar rotation imposes a 27-day recurrence tendency to those ionospheric phenomena that are associated with the emission of particles. Periods shorter than solar rotation period, spectral peaks at about half the solar rotation period, 13-14 days, have persistently appeared in studies of geomagnetic activity using global indices (Fraser-Smith, 1972; Delouis and Mayaud, 1975).

It is clear that the 13.5-day periodicity exists for most solar, heliospheric and geomagnetic variables (Mursula and Zieger, 1996). The amplitude variations of the oscillations in the ionospheric and solar parameters suggest a possible solar ionization influence on ionospheric parameters. So the quasi-periodic oscillations present in the ionospheric electron and ion temperatures can be used to infer the source of heating at the upper ionosphere and the processes existing at those altitudes. Ionospheric electrons are not, in general, in thermal equilibrium with the ion and neutral gases in the F-region and plasmasphere (Brace and Theis, 1981).

Ionospheric electrons are heated preferentially by photoelectrons produced in the lower F region by the absorption of solar extreme ultraviolet radiation and some of these photoelectrons escape to heat the entire plasmasphere (Mantas et al., 1978). Results of studies based on *in situ* measurements and comparisons with the existing ionospheric models on the spatial and temporal variations of electron density and temperature are available in the literature ( Su et al., 1995, ; Watanabe et al., 1995; Bhuyan et al., 2002; Chao., et al., 2003; Niranjana et al., 2003). The electron and ion temperatures at the upper ionosphere depends on solar activity level and is found to exhibit diurnal, seasonal, altitudinal and latitudinal variations (Brace et al., Mahajan, 1967, 1967; Bilitza, 1991; Oyama et al., 1996a; Otsuka et al., 1998; Bhuyan et al., 2002).

The electron temperature was found to exhibit a sharp predawn enhancement, a daytime trough, evening enhancement and stable night-time value. A number of local and non-local processes can affect the low latitude thermosphere. Periodic fluctuations in the geomagnetic activity and ionospheric fluctuations result from the intrinsic state of the Sun, relative orientation of the Earth with respect to the Sun, evolution of solar surface features and interplanetary medium and processes at the earth (Nayar et al., 2001,2002). Here the electron and ion temperature using the RPA payload of the SROSS C2 satellite during 1995 to 2000 of the low latitude upper ionosphere have been evaluated. The data has been separated in to two time series representing day time and night time. It is then used to investigate the periodicities present in them and their association with solar and terrestrial processes. The temporal evolutions of these periodicities were also studied using the wavelet technique.

## 2. Observations and Data Analysis

The data analyzed here is derived from SCROSS-C2 RPA and from 1995 to 2000. The data is then separated in to day time and night time average values by averaging the  $T_e$  and  $T_i$  measurements made during the visibility period. This is a period of rising phase of solar activity. The daily average of day time refers to the average of measurements taken between 1000 and 1600 LT and night time values refers to the measurements taken between 2000 to 0400 LT, discarding the data around morning overshoot and evening enhancement. The data gaps, when the satellite pass is outside the above mentioned time slots are then filled using interpolation. For the evaluation of day time and night time average values of  $T_e$  and  $T_i$ , data from the entire range of latitude, longitude and altitude covered by SROSS C2 satellite is used. Thus these values are mixed with seasonal, altitudinal, latitudinal, longitudinal and solar cycle effects. From the daily daytime and nighttime average values, a time series of  $T_e$  and  $T_i$  are generated. The electron and ion temperatures corresponding to daytime and nighttime are depicted in Figures 1 and 2. This data is subjected to both Fourier and wavelet analysis to identify the presence of periods and their time evolution. The periodic variation of all the phenomena can be obtained by using spectral analysis. The powerful techniques of spectral analysis developed and based up on the fast Fourier transform (FFT) make possible a detailed search for periodicities in the time variation of  $T_e$  and  $T_i$ . By using the technique of wavelet analysis wavelet spectrum and the global wavelet spectrum of the electron and ion temperatures were obtained.

## 3. Periodicities in SROSS-C2 RPA Data of $T_e$ and $T_i$

The electron and ion temperature observed at the upper ionosphere using the RPA payload of SROSS-C2 satellite exhibits a variety of variations. These variations include diurnal variations with morning overshoot, day time plateau,

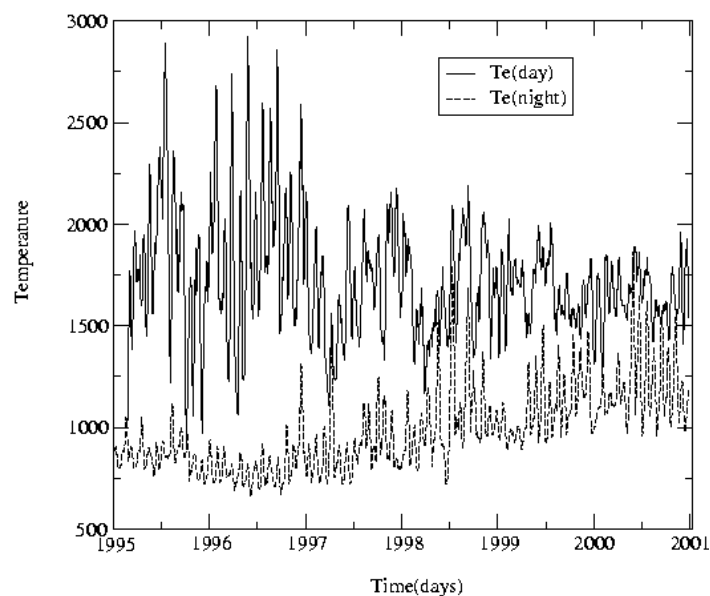


**Figure 1:** Day-time (full line) and night- time (dotted lines) average values of electron temperature during 1995-2000

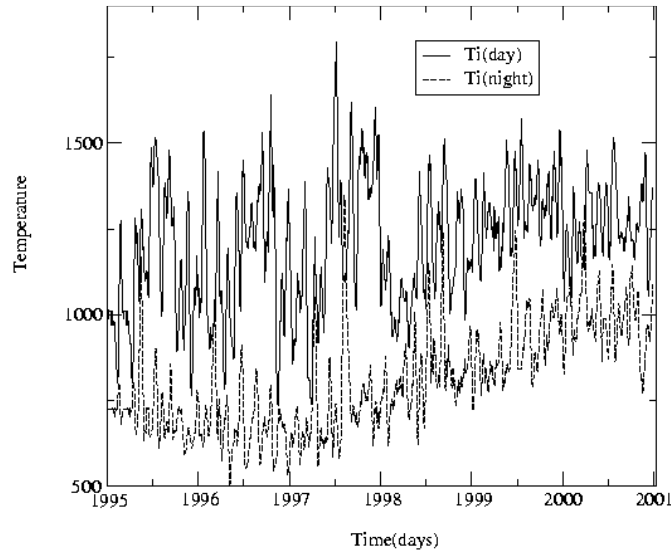


**Figure 2:** Day-time (full line) and night- time (dotted lines) average values of ion temperature during 1995-2000 Evening enhancement and nighttime minimum, 27-day solar rotation associated changes, seasonal variations and solar activity related variations. To study the periodicities present in these fluctuations and to probe in to the sources of fluctuations in electron and ion temperatures and to study the periodic variations in  $T_e$  and  $T_i$ , the time series of the day time and night-time average values were subjected to both FFT and Wavelet analysis. While the Fourier technique provides information about the average power of each period, the wavelet technique provides the time history of each period. The wavelet transform method gives good information on the time location of each frequency component. The global wavelet spectrum, similar to Fourier transform technique, provides information about the mean strength of each periodicity over the entire period of analysis.

**4. Fourier Spectrum of  $T_e$  and  $T_i$**

The periodic variation of all the phenomena can be obtained by using spectral analysis. The powerful techniques of spectral analysis developed and based upon the fast Fourier Transform make possible a detailed search for periodicities in the time variation of  $T_e$  and  $T_i$ . The daily averaged values of  $T_e$  and  $T_i$  during day-time and night-time are separated to two time series representing day-time and night-time values over the period 1995-2000 and are subjected to Fourier analysis after de-trending the data and the power Lomb periodograms (Press et al., 2000) are obtained.

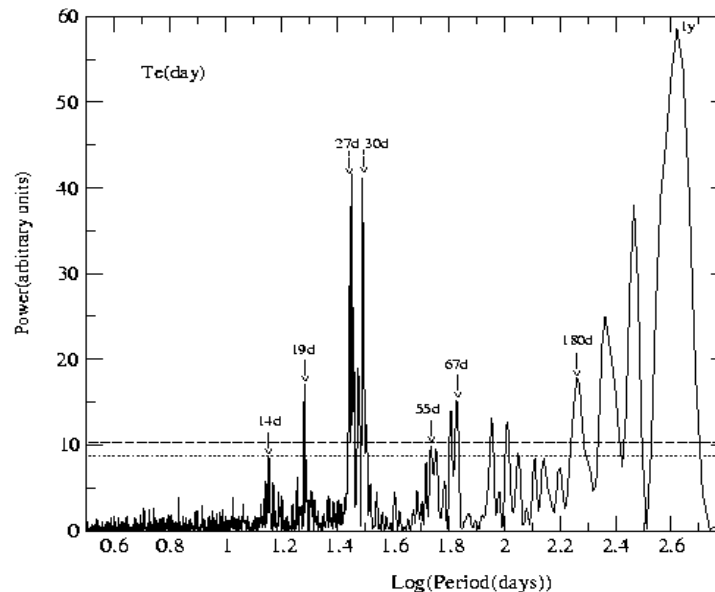


**Figure 3:** Periodograms of daytime electron temperature

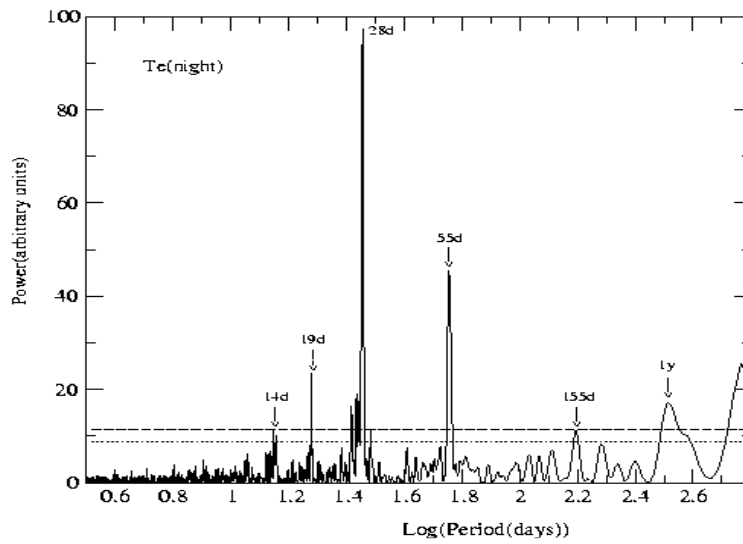


**Figure 4:** Periodograms of daytime electron temperature

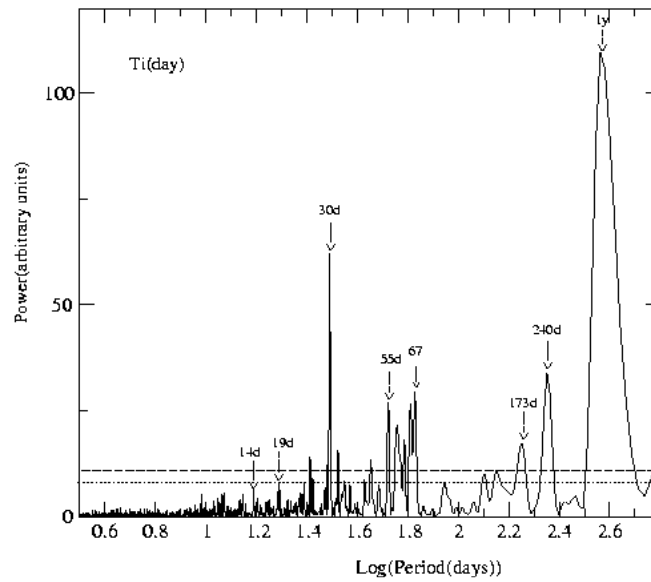


**Figure 5:** Periodograms of daytime ion temperature

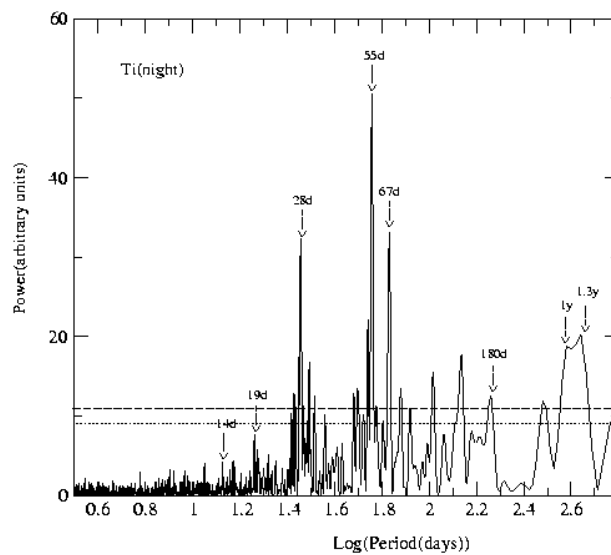


**Figure 6:** Periodograms of nighttime ion temperature

The Figures from 3 to 6 depict the periodograms of electron and ion temperatures of the time series of day-time and night-time averages in the period range, a couple of days to 1.73 years. The numbers in figures 3 to 6 indicate the corresponding period in days. Figure 3 depicts the spectrum of the electron temperature averaged over the nighttime observations at the upper ionosphere around 500 km altitude. The Y-axis represents the spectral power in arbitrary units and the X-axis depicts the log of period in days. The dashed upper line in figure 3 is the upper limit of the 90% confidence level and lower dotted line corresponds to the upper limit of 50% confidence level.

In figure 3, the day time values of  $T_e$  depicts a variety of spectral peaks in the power corresponding to periods around 14-day, 19-day, 27-day, 30-day, 55-day, 67-day, 180-day and about 1.1 year. The 27-day period is associated with the solar rotation and the 55-day period is associated with the harmonic of solar rotation period. The cause of 30-day period is not yet known and it may be associated with the evolution of solar activity or with the planetary wave activity. 14-day period is associated with the presence of active centers on the solar surface separated by 1800 longitude. 13.5-day periodicity exists for most solar and geomagnetic variables not all the time but rather as a quasi periodicity during certain specific intervals. The source of 19-day period is yet to be clearly understood. It can be either due to the solar activity variation or associated with the planetary wave activity. The 155-day period is associated with the Rieger period (Rieger et al., 1984) observed in solar flares.

The annual oscillation is also prominent in the daytime  $T_e$  values. Figure 6.4 depicts the spectrum of nighttime electron temperature fluctuations. Unlike the spectrum of daytime electron temperature, the nighttime electron temperature exhibits period with very sharp periods around 14-day, 19-day, 27-day, 55-day, 155-day and one year. Most of the spectral peaks are above the 90% confidence level. In Figure 4 corresponding to the nighttime electron temperature, less number of spectral lines are noticed compared to the spectrum of daytime  $T_e$ . In Figure 4, the spectral peaks around 14-day, 19-day, 27-day, 55-day, 155-day, 1-year are clearly seen as prominent lines above the confidence level.

Figures 5 and 6 depict the spectrum of  $T_i$  associated with day time and night-time values. The spectrum of  $T_i$  also exhibits few sharper spectral lines above the noise level both during daytime and nighttime. While the 30-day period is prominent oscillation  $T_i$  during daytime, the 28-day period is prominent in the nighttime data. The 55-day, 180-day and 1-year periods are found in both daytime and night time  $T_i$  data. The 1.3-year period is very prominent in the night time  $T_i$  data. However, in all data sets the spectral lines are very broad around 1-year period.

## 5. Wavelet Spectrum

Wavelet analysis is a tool for analyzing localized variations of power within a time series (Lau and Weng, 1995; Torrence and Campo, 1998; Nayar et al., 2002). By decomposing a time series in to time frequency space, wavelet transform has been used in a variety of fields and was found advantageous compared to the conventional tools for time series analysis. In the wavelet theory we use wavelets which are special signals having amplitudes of definite duration and with specific frequency, which decay to zero in both positive and negative directions. Sets of wavelets are used to approximate a signal similar to the case of Fourier series and each element in the wavelet is constructed from the same function called mother wavelet, which is scaled and translated. Wavelet transform refers to the breaking down of the time series in to many inter related components. The scaling and translations are done simultaneously on the mother wavelet functions. The mother wavelet is the kernel of the wavelet transform from which a set of scaled and translated wavelets are created.

The discrete wavelet transform is defined with respect to mother wavelet  $\psi$ . After fixing the width of the wavelet, we can measure the projection of this wave packet on the time series data. i.e., by sliding the wavelet along the time series we can determine the variation of projection amplitude with time. The choice of the wavelet function  $\psi(\eta)$  at non-dimensional time  $\eta$  is made after considering its suitability for the application. In this analysis, we have used Morlet wavelet which is defined as the product of a complex exponential wave and a Gaussian envelope. The value of wavelet transform can be calculated for various values of the scale, which is usually taken as the multiple of lowest frequency possible. A two dimensional plot of the variability can be constructed by plotting the wavelet amplitude and phase.

For the present study we have used Morlet wavelet defined as

$$\psi_0(\eta) = \pi^{-1/4} e^{i\omega_0\eta} e^{-\eta^2/2} \quad (1)$$

where  $\omega_0$  is the wave number taken to be 6. In the case of Morlet wavelet for  $w_0 = 6$ , the Fourier period is 1.03 times the wavelet period (Torrence and Campo, 1998).

If the wavelet power spectrum is significantly above the mean power spectrum, then it can be assumed to be true factor with a certain percent confidence. For the present analysis used the  $T_e$  and  $T_i$  data of the upper ionosphere observed by the RPA payload of SROSS-C2 satellite. The data  $T_e$  and  $T_i$  is available during 1995-2000 as daily average values daytime and night-time separately. From these parameters, both global spectra and scalograms are obtained to study the periods in them and to understand the evolution of periodicities with time. The global wavelet spectrum is similar to the Fourier spectra, giving the average strength of each period during the entire range of observation period. The scalogram provides information about the evolution of the power associated with each period. Here the analysis is restricted to periods above 10 days to 2 years.

### 5.1 Global Wavelet Spectra of $T_e$ and $T_i$

In this section, the presence of periodicities in electron and ion temperatures in the upper atmosphere has been analyzed by wavelet technique by looking at their temporal average behavior using global wave spectrum. The global wavelet spectrum is the plot of mean wavelet power against wavelet period. In this case, since we use Morlet wavelet, the wavelet scale/period is nearly equal to Fourier period. So the global spectrum is similar to the Fourier spectrum with the wavelet period and Fourier period differing depending on the selection of wavelet. In figures 7 and 8, the upper dashed lines indicate the 90% confidence level and the lower dashed lines indicate the 50% confidence level of the red noise background spectrum (Torrence and Campo, 1998). Most prominent periods present in the global wavelet spectra of electron and ion temperature are around 27-day, 55-day, 154-day and 1-year. The global wavelet spectra of  $T_e$  (day),  $T_e$  (night),  $T_i$  (day) and  $T_i$  (night) in the period range 1-day (0.05) to 3-year (3.2) are depicted in Figures 7 and 8. The upper curve in figure 7 depicts the global wavelet spectrum of nighttime  $T_e$  and lower curve depicts the daytime  $T_e$ . As in the case of Fourier spectra, the 27-day and 55 day periods are prominent in  $T_e$  nighttime data. Similarly for  $T_e$  at daytime (Figure 7 lower) 27-day and 1-year periods are prominent and seen above the noise level. The upper graph in figure 8 indicates the global wavelet spectra of nighttime  $T_i$  data and the lower portion depicts the global spectrum of  $T_i$  during day time. In the case  $T_i$  data,

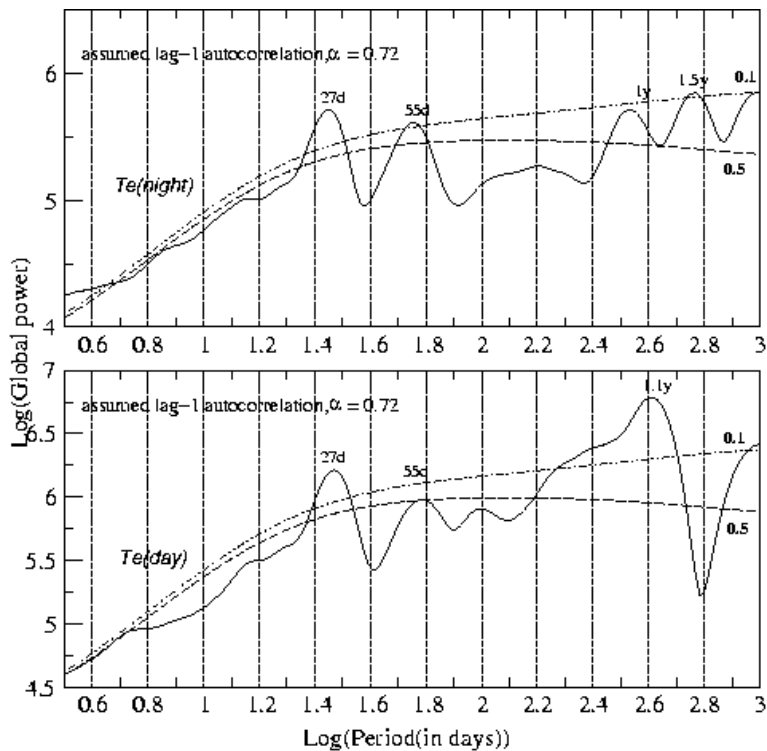


**Figure 7:** Global wavelet spectra of average value of electron temperature during daytime and that of nighttime. The dotted line indicates the 90% Confidence level and dashed line indicates the 50% confidence level of the Red noise background spectrum

Both during day-time and night-time the 27-day, 55-day and 1-year wavelet periods are seen above the 90% confidence level. Since the global wavelet spectra are the time average of the wavelet power during different epochs, the spectral peaks are broader and many spectral peaks are vanished below the confidence level.

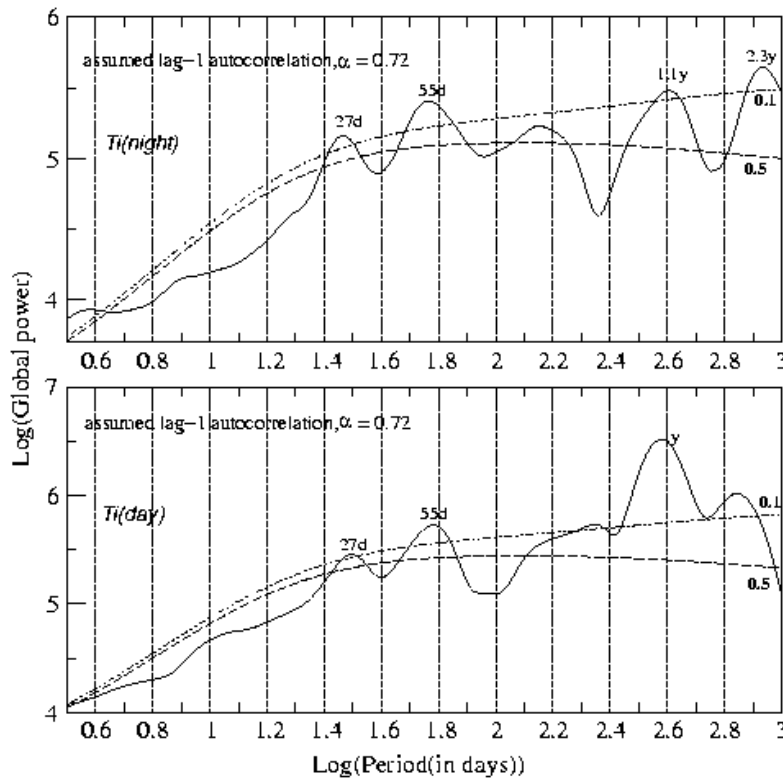


**Figure 8:** Global wavelet spectra of average value of ion temperature during daytime and that of nighttime. The dotted line indicates the 90% Confidence level and dashed line indicates the 50% confidence level of the Red noise background spectrum

**5.2 Wavelet spectrum of Te and Ti**

Figures 9 to 12 depict the wavelet spectra of Te and Ti during day-time and night-time. The wavelet spectrum is a periodogram depicting the evolution of wavelet power with time. Since we use Morlet wavelet for the present analysis, the wavelet period is nearly the same as that of Fourier periods in Figures 9 to 12. The wavelet power is not evenly distributed in the periodogram. The power is concentrated at certain period bands and is found to evolve with time.

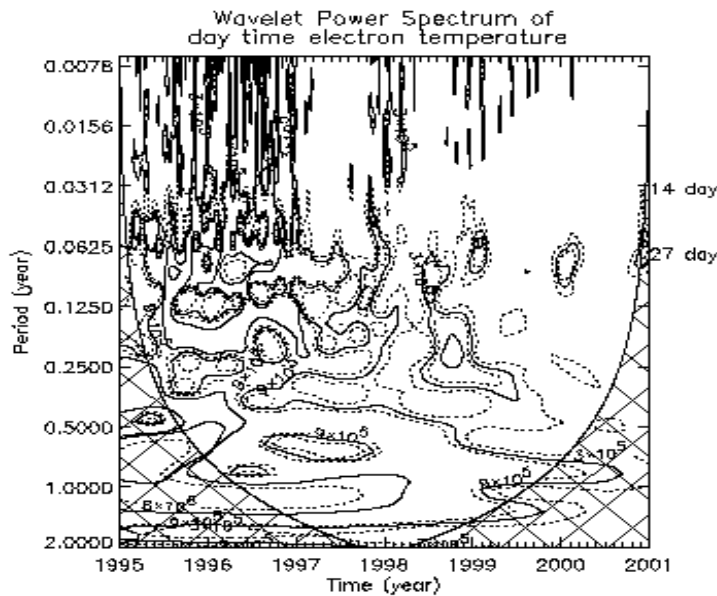


**Figure 9:** Wavelet spectra of electron temperature during day-time.

The wavelet scale is marked in year along y-axis. The power corresponding to each contour is marked in figures. The mesh indicates the regions where the edge effect becomes important.

Since the data used is not cyclic, to minimize errors at the beginning and end of the wavelet spectrum, the time series of  $T_e$  and  $T_i$  are padded with zeros to bring the data length to power of two. This introduces decrease in amplitude at the end points as one goes to larger scales. The region indicated by the mesh indicates the region of the spectrum in which edge effects become important. Figure 9 depicts the time history of the wavelet power of the fluctuations in the daytime  $T_e$  during 1995-2000.

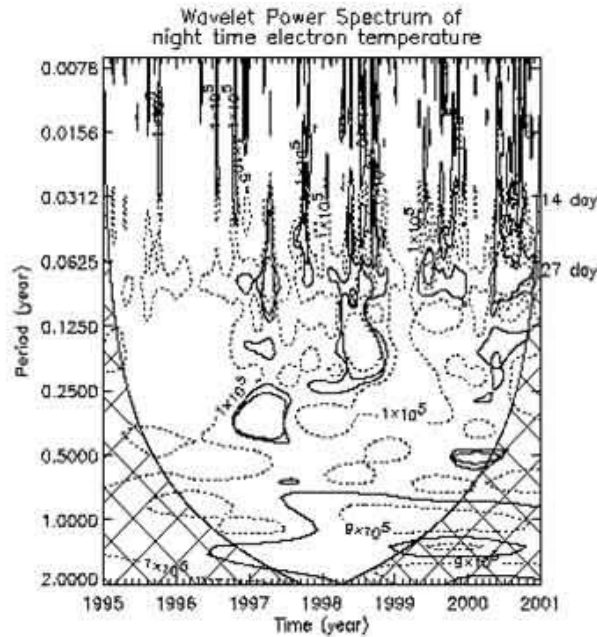


**Figure 10:** Wavelet spectra of electron temperature during night-time. Other details same as Figure 9

It is noticed that during 1995-97, most of the periods exhibit larger wavelet power compared to later years. The 14-day period has larger power around 1996 and 19-day period around 1995-96. The 27-day, 55-day, 180-day and 1 to 1.3-year periods are prominent during the three years 1995-97.

In Figure 10 depicts the time evolution of the wavelet power of average night-time electron temperature. Unlike the day-time  $T_e$  data, night-time  $T_e$  data

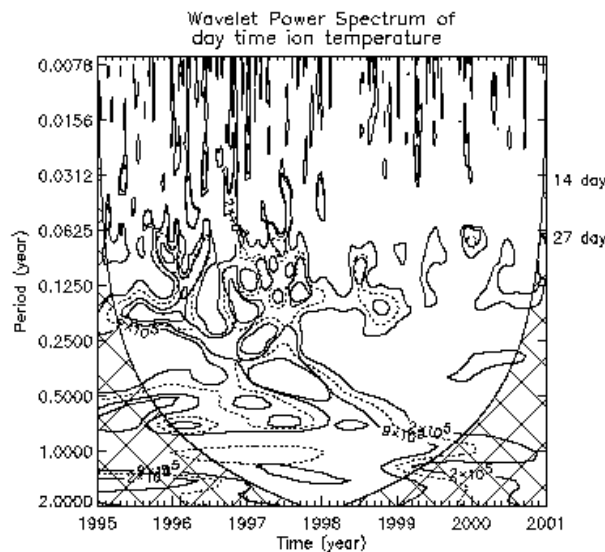


**Figure 11:** Wavelet spectra of ion temperature during day-time. Other details same as Figure 9



Exhibit larger wavelet power during the period 1997-2000 for 14-day, 19-day, 27-day, 180-day and 1-year periods. The wavelet powers of short period oscillations around 14-day, 19-day and 27-day show periodic variations in their strength during the period. During 1998, the wavelet power is found to be stronger below 100-day period.

Figure 11 depicts the time history of the wavelet power of ion temperature during daytime. The 27 and 55-day periods are stronger in the ion temperature with a peak wavelet power around 1996-97. The periods around 55-day is prominent during 1997. The 180-day and 1-year also exhibit maximum power around 1995 to 1997. During 1997, the wavelet power enhances around 1.3year period

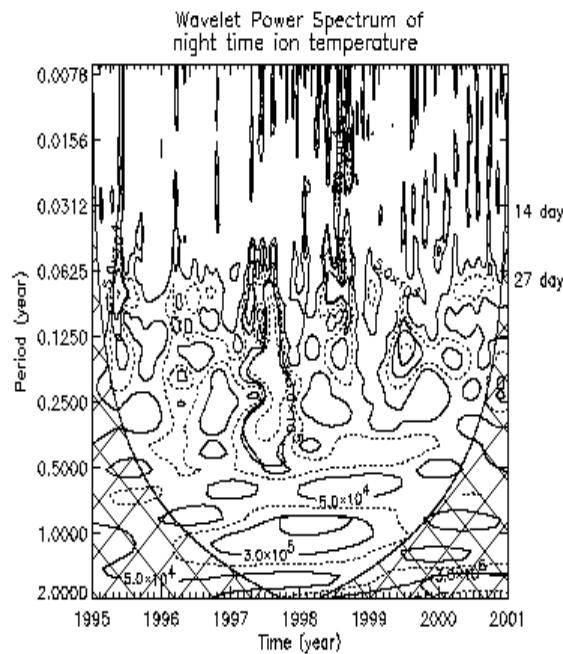


**Figure 12:** Wavelet spectra of ion temperature during nighttime. Other details same as Figure 9

Figure 12 depicts the temporal evolution of the wavelet power of ion temperature at nighttime. The wavelet spectra of  $T_i$  at night exhibit peak values around 1995, 1997 and 1998. Similarly the wavelet power of 55-day period also exhibits intermittent increase in wavelet power. The 180-day period is found to be prominent during 1997-99. A strong enhancement in the wavelet power is noticed in a narrow time period around 1997 in the period range 27 day to 180 day.

### 6 .Wavelet Spectrum of $A_p$ and F10.7 Flux and Cross-Spectrum with Electron and Ion Temperatures

To identify the cause of periodic fluctuations in the daytime and nighttime  $T_e$  and  $T_i$  and their association with solar activity, here studied the wavelet spectra of the geomagnetic activity index  $A_p$  and solar radio flux F10.7. The geomagnetic activity index  $A_p$  is directly related to the solar wind velocity and the solar radio flux is an indicator of solar activity and sunspot number. Figure 13 and 14 depict the time evolution of wavelet power for different periods in  $A_p$  index and F 10.7 .

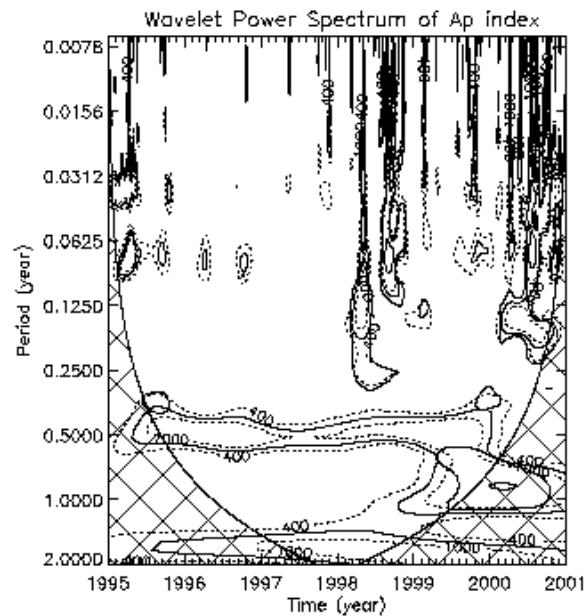


**Figure 13:** Wavelet spectra of Ap index during 1995-2000. Other details same as Figure 9

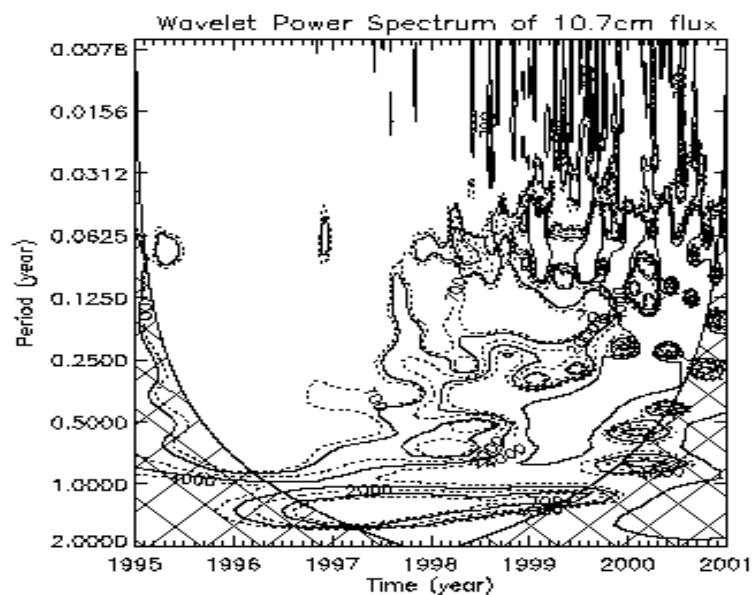


**Figure 14:** Wavelet spectra solar radio flux F10.7 during 1995-2000. Other details same as Figure 9

The Ap index exhibits larger wavelet power associated with semi-annual period during 1995-99 and around 1-year period during 2000. Due to poor resolution, the 155-day period is merged with in the semi-annual period band and the 1.3 year period is merged with in the I-year band. The 14-day and 27-day period in Ap are prominent during 1995-96. During 1998 and 2000 most of the short period oscillations in the period band less than 100-days exhibit larger wavelet power. Compared to the Ap index, the F10.7 index depicts larger wavelet power during 1998-2000 and wavelet power is found to be highly evolving during this period without the dominance of any particular period.

For a quantitative evaluation of the relation between the wavelet powers of Te and Ti with Ap index and F10.7 index, the cross wavelet power is evaluated for a typical period of 27-day. Figure 15 depicts the cross wavelet power between Ap index and the electron temperatures at daytime Te (d) and night-time Te (n) and ion temperatures at day-time Ti (d) and night-time Ti (n) during 1995-2000 expressed in days. The relation between the Ap index and the ionospheric temperatures at

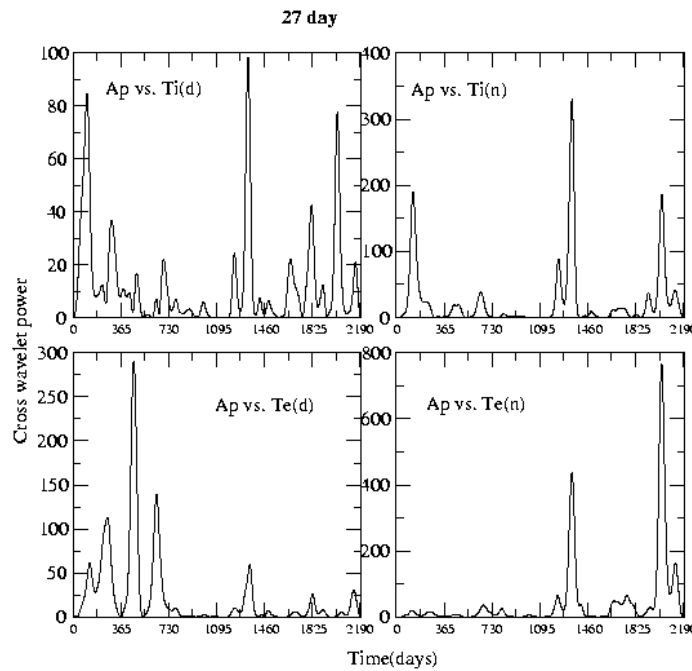


**Figure 15:** Time evolution of cross wavelet spectrum between Ap and electron and ion temperatures for the 27-day periodicity during 1995 - 2000 (marked as days along x-axis)

27-day period is found to be stronger during the solar minimum years 1995-96. During 1998 a prominent enhancement in the cross wavelet power is noticed. In the case of cross wavelet power between F10.7 index and electron and ion temperatures during 1995 - 2000 is as depicted in Figure 16. It is noticed that in general the cross wavelet spectrum is stronger during 1998-2000, indicating that the wavelet power of 27-day wavelet scale in Te, Ti and F10.7 are well correlated during 1998-2000.

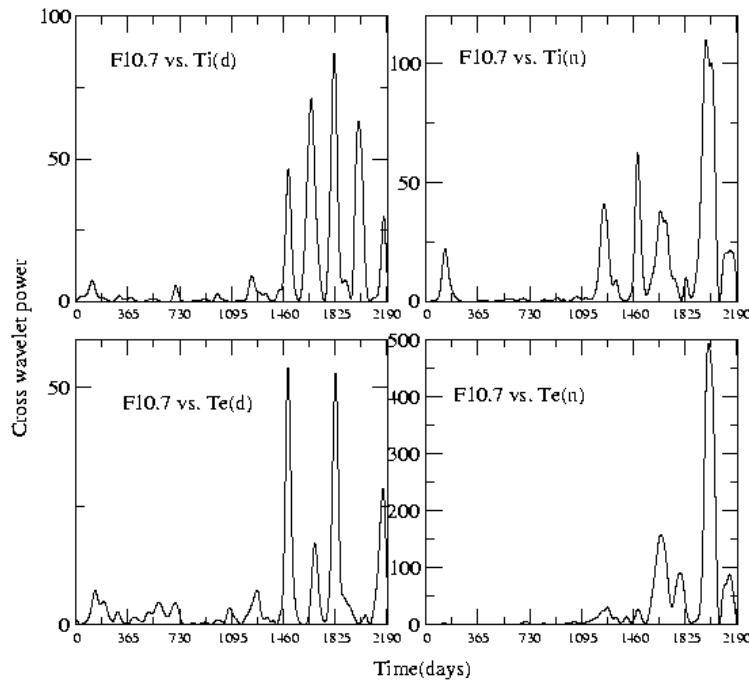


**Figure 16:** Time evolution of cross wavelet spectrum between solar radio flux and electron and ion temperatures for the 27-day periodicity during 1995-2000 (marked as days along x-axis)

### 7. Temporal Evolution of Wavelet Power

To identify prominent periods and study the time evolution of certain prominent periods, the variation of wavelet power associated with 13.5-day, 19-day, 27-day and 155-day periods are depicted Te (day and night separately),

Ti (day and night), Ap and 10.7radio flux in Figures 17, 18 and 19. Figure 17 left column depicts the time variation of wavelet power associated with daytime Te. The wavelet power of Te-day is larger during 1995-1997 compared to later years. This result is comparable with that presented in Figure 9. Whereas for the night-time Te values of wavelet power, as seen on the right column of Figure 17, is peaking beyond 1997 for periods 13.5, 19 and 27 days. Figure 18 depicts the time variation of wavelet power with time for the ion temperatures at

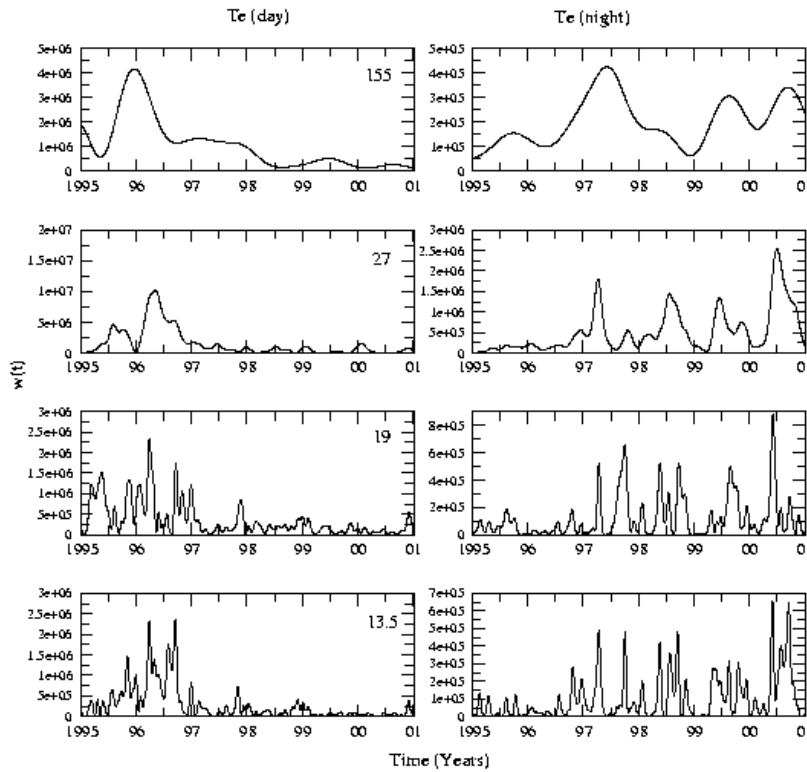


**Figure 17:** Time variation of wavelet power of Te during day time and night time for few periods

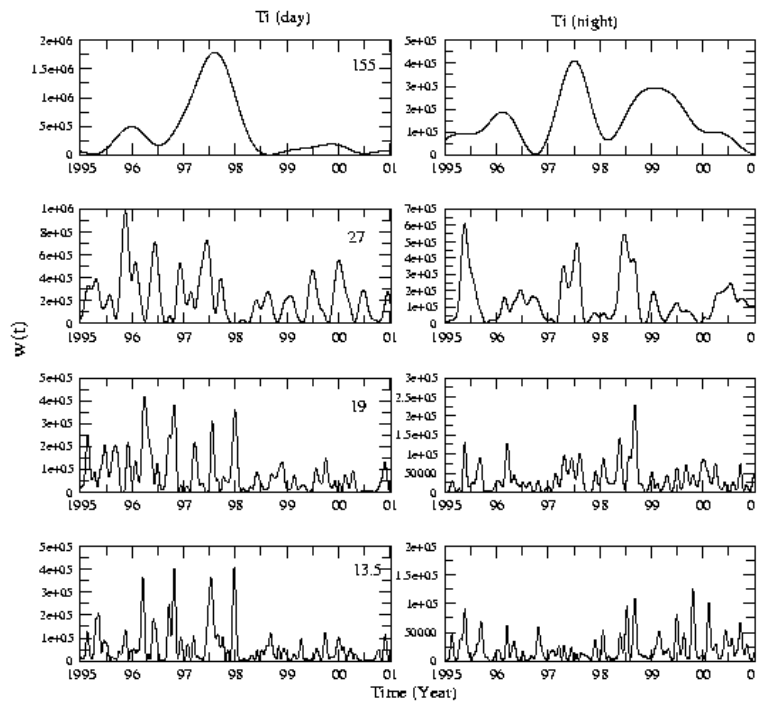


**Figure 18:** Time variation of wavelet power of Ti during day-time and night-time for few periods

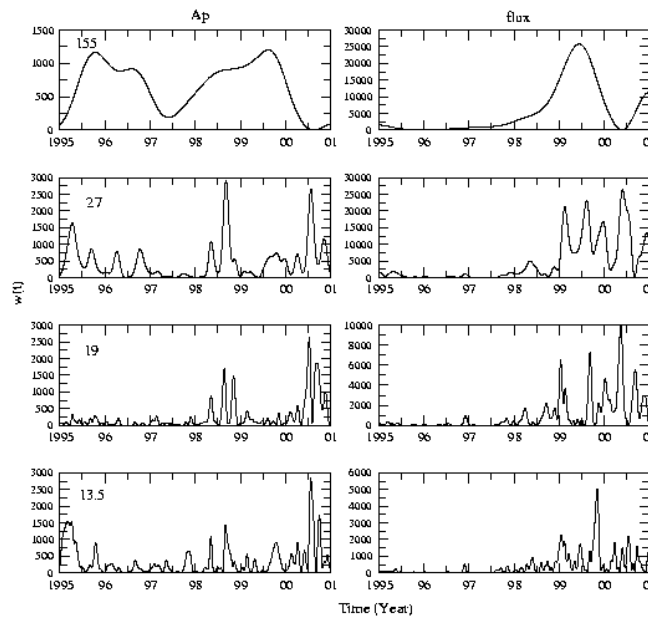


**Figure 19:** Time variation of wavelet power of Ap index and the F10.7 cm radio flux

day-time and night-time. The wavelet power for the day-time  $T_i$  has larger power around 1995-1998 period for all the periods presented in Figure 18, similar to that of  $T_e$ . In the case of night time  $T_i$  the wavelet power is evenly distributed throughout the period considered in this work.

Figure 19 depicts the time variation of the wavelet power for few periods in the Ap index and the 10.7 cm solar radio flux. It is noticed that both the Ap index and the 10.7 flux have their wavelet power evolving with time similar to that of night time  $T_e$ .

## 8. Discussion

In this work, the periodicities present in the electron and ion temperatures at the low latitude topside ionosphere in the altitude around 500 km have been studied. The electron and ion temperatures at the low latitude topside ionosphere are evaluated from the observation of I - V characteristic curves obtained using RPA payload onboard the SROSS C2 satellite and are separated into day-time and night-time average values for each day and presented in Figures 1 and 2. The characteristics of these fluctuations in  $T_e$  and  $T_i$  studied using Fourier and wavelet techniques provide complementing information. While the Fourier spectra presented in Figures 3- 6 depicts the Fourier power corresponding to periods 14-day, 19-day, 27-day, 55-day, 155-day, 180-day, 1-year and 1.3year. The Fourier spectrum give information about the power for the entire period, the wavelet analysis (Figures 7 to 12) provides information about their time history during 1995-2000. The presence of these periods in electron and ion temperatures along with other solar and terrestrial parameters (Nayar et al., 2002) gives an indication of the sources of heating at the upper ionosphere.

The source of 14-day periodicity is the presence of two active centers on the solar surface separated by 1800 solar longitude. The F10.7 radio flux is characterized by a small 13.5-day peak and largest 13.5-day periodicity recorded by 2050-A0 fluxes. Examining the periods shorter than solar rotation period 13-14-day periodicity have persistently appeared in studies of geomagnetic activity using global indices ( Fraser-Smith, 1972; Delouis and Mayoud, 1975) and, in the Sun, Solar wind and geomagnetic activity ( Mursula and Zieger, 1996). Donnelly and Puga (1990) found that the power of the 13.5-day periodicity is very dependent on the wavelength or source region. A strong overall power in 13.5-day periodicity was found in ultraviolet (175-290 nm) and the power and phases of the 13.5-day periodicity at the various wavelengths in terms of their optical depth and solar central angle dependence. This strong periodicity comes from episodes of solar activity with two peaks per rotation, produced by two groups of active regions roughly 1800 apart in solar longitude and verifying the earlier work by Heath (1973) in UV and other variables and indices (Donnelly et al., 1983; 1985; Lean, 1984; Bai, 1987).

The 27-day period is associated with the solar rotation and the 55-day period with its harmonics. The 154-day period is called the Rieger period associated with the recurrence of solar flares and in different aspects of solar activity study (Delache et al., 1985; Lean and Brueckner, 1989; Bai and Cliver, 1990).

The 1.3-year period is associated with the evolution of solar rotation is found in many solar and interplanetary parameters. These periods affect both the solar radiation output and the characteristics of the outflow of solar wind and interplanetary magnetic field. The annual and semiannual periods are associated with the solar terrestrial relation found in many terrestrial activity indices. The wavelet spectra of Ap and F10.7 indices evaluated for the period 1995-2000 (Figures 13 and 14) enables one to compare similar features in these indices and the ionospheric plasma temperatures. The cross wavelet spectrum presented in Figures 15 and 16 indicates the temporal evolution of the relation between them.

The ionospheric variations are influenced by changes of solar ionizing radiations, variations in solar wind plasma parameters and other variations due to vertical transport of planetary wave energy generated at the lower atmosphere. The electron and ion temperature at the upper ionosphere is also affected by the electric field variations and the related density changes. The study of the characteristics of the Fourier and wavelet spectrum helps us to infer the prominent processes associated with the heating of the upper ionosphere. Most of the periods present in Te and Ti are associated both with the solar wind and solar radiation and is associated with active centers at the solar surface. Though some of the periods have their Fourier power below the significant level, the wavelet spectrum indicates their prominence during certain epochs. The study of the similarities of the time evolution of wavelet power of Ap and F10.7 indices with Te and Ti and the cross wavelet spectrum indicate that the plasma temperature at the upper ionosphere is controlled by solar wind around the solar minimum and by both the solar radiation and solar wind around solar maximum. These results suggests that the processes associated with the heating of ionospheric plasma by the solar radiation and the solar wind depends on the phase of the solar cycle and the conditions of the solar radiation, interplanetary medium and magnetosphere.

The periodicity around 19-day observed in the Te and Ti spectrum can be utilized to study the possible contribution of planetary waves generated at the lower atmosphere on the upper ionosphere temperature. In the spectrum of electron and ion temperatures, the 19-day period is having significant spectral power. The wavelet spectrum of Ap index and F10.7 do not exhibit this periodicity. Dynamical coupling through various types of waves generated at the lower altitudes play an important role in the energy transport between lower and upper atmosphere. These waves grow in amplitude as they propagate to higher altitudes and carry significant amounts of energy and momentum to be able to affect the thermospheric heights (Krishna Murthy, 1998).

Even though planetary waves are unable to propagate directly to upper ionosphere, planetary wave type oscillations have been observed at these heights. The 18-day quasi period exists and persists in the ionospheric electron density variations with mean period around 18-19 days (Altadill, 1996). The 18-day quasi periodic oscillation is also present in solar parameters Rz, F10.7 with a mean period around 19-20 days (Wilson, 1982). These results indicate that the period around 19 day can have contribution from solar and terrestrial activities. So, the quasi-periodic oscillations present in the ionospheric electron and ion temperatures can be used to infer the source of heating at the upper ionosphere and the processes existing at those altitudes.

## **9. Conclusion**

From the results obtained it can be concluded that quasi-periodic oscillations exists and persists in the ionospheric electron and ion temperatures. These oscillations are found to be existing in some solar and geomagnetic variables, indices and planetary waves. The spectral analysis of electron and ion temperatures exhibits the presence of variety of periodicities like 14-day, 18-day, 27-day, 31-day, 55-day and 154-day. 27-day periodicity is considered to be of solar origin whereas 14-day periodicity is related to geomagnetic activity. 18-day periodicity obtained suggests a possible solar and planetary wave influence on this oscillation. 55-day and 155- day possess the signature of solar flares. On comparing the periodic variations of electron and ion temperatures with geomagnetic activity and F10.7 solar flux it is found that the peaks around 27-day periodicity is very prominent than peaks around 13.5-day periodicity. 19-day periodicity is prominent in solar flux fluctuations whereas very weak in geomagnetic activity.

So periodicities less than solar rotations may be due to geomagnetic activity, interplanetary magnetic field and planetary wave effect. The spectral analysis of periodic oscillation becomes more effective only by a large database including different solar cycles. We observe similar periodicities in the geomagnetic activity, solar flux, electron and ion temperatures, they indicate the presence of some global periodic phenomena. The amplitude variations of the oscillations in the ionospheric and solar parameters suggest a possible solar ionization influence on ionospheric parameters. So the quasi-periodic oscillations present in the ionospheric electron & ion temperatures can be used to infer the source of heating at the upper ionosphere and the processes existing at those altitudes.

**References**

- Altadill, D, 1996. On the 18 day quasi-periodic oscillation in the ionosphere, *Annales Geophysicae*, 20: 807-815.
- Bai, T and Cliver, E.W, 1990. A 154 day periodicity in the occurrence rate of proton flares, *Astrophysics Journal*, 363: 299.
- Bai,T., 1987. Distribution of flares on the Sun: superactive regions and active zone of 1980-1985, *Astrophysics Journal*, 314, 795-807.
- Bhuyan,P.K., Chamua, M., Subrahmayam ., P and Garg, S.C., 2002, Diurnal, seasonal and latitudinal variations of electron temperature measured by the SROSS C2 satellite at 500 km altitude and comparison with IRI, *Annales de Geophysicae*, 20: 807-815
- Brace, L.H., Theis, R.F., and Hoegy, W.R., 1987, Ionospheric electron temperature at solar maximum, *Advances in Space research*, 7: 99-106
- Bilitza, D., 1991, Electron and ion temperature data for ionosphere modelling, *Advances in space Research*, 11: 10(139)- (10)148
- Brace, L.H and Theis, R.F., 1981, Global empirical models of ionospheric electron temperature in the upper F region and plasmasphere based on in situ measurements from the Atmosphere Explorer-C, ISIS-2 satellites, *Journal of atmospheric and Terrestrial physics*, 43: 1317-1343
- Brace behaviour of the Ionosphere 1000 km a, L.H., Reddy, B.M and Mayr, H.G., 1967, Global latitude, *Journal of Geophysical Research*, 72: 265-283
- Chao, C.K., Su, S.Y and Yeh, C, 2003, Presunrise ion temperature enhancement observed at 600 Km low- and mid-latitude ionosphere, *Geophysical Research Letters*, 30 (4): 36-(1-4)
- Delouis, H., and Mayaud, P.N., 1975. Spectral analysis of the geomagnetic activity index aa over a 103 year interval, *Journal of Geophysical research*, 80, 4681-4688.
- Delache, P; Laclare, F and Sadsaoud, H, 1985. Long period oscillations in solar diameter measurements, *Nature*, 317: 416-418.
- Donnelly, R.F., and Puga, L.C., 1990. Thirteen day periodicity and the centre-to-limb dependence of UV, EUV and X-ray emission of solar activity, *Solarphysics*, 130, 369-390.
- Donnelly, R.F; Heath; D.F., Lean, J.L and Rottman,G.J, 1983. Differences in the temporal variations of solar UV flux, 10.7-cm solar radio, sunspot number and Ca-K plage data caused by solar rotation and active region evolution, *Journal of Geophysical research*, 88, 9883-9888.
- Donnelly, R.F;Harvey, J.W; Heath, D.F and Repoff, T.P, 1985. Temporal characteristics of the solar UV flux and He I line at 1083 nm, *Journal of Geophysical research*, 90,6267-6273.
- Fraser-smith, A.C, 1972. Spectrum of geomagnetic activity index Ap, *Journal of Geophysical research*, 77: 4209-4220.
- Heath, D.F., 1973. Space observations of the variability of solar irradiance in the near and far ultraviolet, *Journal of Geophysical research*, 78, 2779-2792.
- Huba, J.D; joyce, G and Fedder, J.A, 2000a. SAMI2 ( Sami2 is Another Model of the Ionosphere, *Journal of Geophysical Research*,105: 23035-23053.
- Krishnamurthy, B.V., 1998. Middle atmosphere-upper atmosphere coupling , *PINSA*,64,303-313.
- Lau, K.M. and Weng, H.Y., 1995, Climate signal detection using wavelet transform: How to make time series sing, *Bull. Amer. Met. Soc.*, 76: 2391-2402.
- Lean, J.L., 1984. Estimating the variability of the solar flux between 200 and 300 nm, *Journal of Geophysical research*, 89, 1-9.
- Lean, J.L and Brueckner,G.E., 1989. Intermediate term solar periodicities : 100-500 days, *Astrophysics Journal*., 337, 568-578.
- Mahajan, K.K., 1967,10.7cm solar radio flux and ionospheric temperatures.*Journal of Atmos. and Terr. Physics*}, 29:1153-1158
- Mantas, G.P., Carlson, H.C and Wickwar V.B., 1978, *Journal of Geophysical research*., 83:1
- Mursula, K and Zieger, B, 1996. The 13.5 day periodicity in the Sun, solar wind and geomagnetic activity: The last three solar cycle, *Journal of Geophysical Research*, 101: 27077-27090.
- Nayar, S.R, Prabhakaran; Radhika, V.N; Ramadas,V and Revathy, K, 2002.Wavelet analysis of periodicities in the interplanetary medium, *Solar Physics*, 208: 359-373.
- Nayar, S.R, Prabhakaran; Sanalkumaran Nair,V; Radhika, V.N and Revathy, K, 2001. Short period features of the interplanetary plasma and their evolution, *Solar Physics*. 201: 405-417.

- Niranjan, K., Sridhar, H.S., Rama Rao, P.V.S, Garg, S.C., Surahmanyam, P, 2003. Evening temperature in F-region electron temperature at subtropical latitudes during June solstice in the Indian SROSS C2 RPA data, *Journal of Atmospheric and Solar-Terrestrial Physics*, 65: 813-819.
- Oyama, K.I; Balan, N; Watanabe, S; Takahashi, T; Tsuda, F; Bailey, G.J and Oya, H, 1996a. Morning overshoot of  $T_e$  enhanced by downward plasma drift in the equatorial topside ionosphere, *Geomagnetism and Geoelectricity*, 48: 959-966.
- Otsuka, Y., Kawamura, S., Balan, N., Fukao, S and Baily, G.J, 1998. Plasma temperature variations in the ionosphere over the middle and upper ionosphere radar, *J. Geophys. Res.*, 103: 20275-20713.
- Press, W.H., Flannery, B.P., Teukilsky, S.A. and Vetterling, W.T, 2000, *Numerical recipes in C, the art of scientific computing*, Cambridge University Press, New Delhi.
- Rieger, E., Share, G.H., Forrest, D.J., Kanbach, G., Reppin, C., Chupp, E.L., 1984. A 154-day periodicity in the occurrence of hard solar flares., *Nature*, 312, 623- 625.
- Schunk, R.W and Nagy, A.F, 2000. *Ionospheres-Physics, plasma physics and chemistry*, Cambridge University Press, Cambridge, U.K.
- Schunk, R.W. and Nagy, A.F., 1978, Electron temperatures of the F-region of the ionosphere-Theory and observations, *Reviews of Geophysics and Space Physics*, 96:355-399
- Su, Y.Z., Bailey, G.J and Balan, N, 1995. Modeling studies of longitudinal variations in TEC at equatorial anomaly latitudes, *Journal of Atmospheric and Terrestrial physics*, 57: 433-442.
- Torrence, C. And Campo G.P; *A Practical guide to Wavelet Analysis*, *Bull. Amer. Met. Soc.*, 79, 61-78, 1998.
- Watanabe, S., Oyama, K.I. and Abdu, M.A., 1995, Computer simulation of electron and ion densities and temperatures in the equatorial F-region and comparison with Hinotori results, *Journal of Geophysical Research*, 100:14581-14590.
- Wilson, R.C.; Solar irradiance variations and Solar activity. *Journal of Geophysical Research*, 87, 4319-4326, 1982